Cement and Concrete Research 40 (2010) 94–101

Contents lists available at ScienceDirect

Cement and Concrete Research

journal homepage: http://ees.elsevier.com/CEMCON/default.asp

New observations on the mechanism of lithium nitrate against alkali silica reaction (ASR)

X. Feng [a,*], M.D.A. Thomas [a], T.W. Bremner [a], K.J. Folliard [b], B. Fournier [c]

[a] Department of Civil Engineering, University of New Brunswick, Fredericton, NB, Canada
[b] Concrete Durability Center, The University of Texas at Austin, TX, USA
[c] Concrete Technology Program, CANMET-MTL, Ottawa, ON, Canada

ARTICLE INFO

Article history:
Received 19 August 2008
Accepted 15 July 2009

Keywords:
Lithium nitrate
Alkali silica reaction (ASR)
Vycor glass
Mechanism

ABSTRACT

In the current study, in order to elucidate the mechanisms for the favorable effects of lithium nitrate in controlling alkali silica reaction (ASR), vycor glass disk immersion specimens and glass disk–cement paste sandwich specimens were prepared and examined by XRD, SEM and Laser Ablation Induction Coupled Plasma Mass Spectrometry (LA-ICP-MS). Results showed that when glass disk was immersed in only NaOH solution, the glass was attacked by hydroxyl ions but no solid reaction product was found, thus the presence of calcium was essential for the formation of ASR gel. In the presence of lithium, the glass surface was covered by a thick layer of Li–Si crystal. With the addition of $Ca(OH)_2$, the glass surface was completely covered by Li–Si crystal and a lithium-bearing low Ca–Na–(K)–Si gel. These two phases either form a dense matrix with Li–Si crystal serving as the framework, and the gel filling in the void space, or the Li–Si crystal serving as the foundation to completely cover the entire reactive SiO_2 surface, and the gel sitting on top of these crystal particles. Hence, the suppressive effects of $LiNO_3$ were attributed to the formation of a layer of Li–Si crystals intimately at the reactive SiO_2 particle surface and the formation of Li-bearing low-Ca ASR gel products. The Li-bearing low-Ca ASR gels may have a dense and rigid structure, thus having low capacity to absorb moisture from the surrounding paste, and exhibiting a non-swelling property.

1. Introduction

Interest in applying lithium-containing compounds to control alkali silica reaction (ASR)-induced expansion was dated back to 1950s when McCoy and Caldwell [1] found that among over 100 different compounds, lithium-containing compounds were the most promising chemicals (LiCl, Li_2CO_3, LiF, Li_2SiO_3, $LiNO_3$, and Li_2SO_4) to mitigate ASR-induced expansion provided they were used in sufficient quantity. Since then, a substantial body of work [2–13] has demonstrated the efficacy of lithium compounds in controlling ASR in concrete.

Several mechanisms have been proposed by different researchers to explain the effect of lithium on reducing expansion. Some are focused on the alteration of the nature of the reaction products yielded in the presence of lithium [2,3], some are focused on the effect of silica dissolution [2,14], or ASR gel repolymerization [15,16], while others are based on colloid and surface chemistry theory [17]. Recently, Thomas [18] suggested that attention should be paid to the role of calcium in the suppressive effects of lithium on ASR-expansion. Based on the discussion about the proposed mechanisms [19,20], it can be said that all of the proposed mechanisms are reasonable under certain circumstances, but there are some findings from the previous work on the influences of lithium on ASR that no mechanism totally explains. For example, why lithium salts are more effective with highly reactive aggregates than with slowly reactive aggregates and what the role of calcium is. Hence, the mechanism(s) responsible for the favorable effects of lithium compounds on reducing ASR-induced expansion has not been unequivocally established [20].

A better understanding of the mechanism(s) will help significantly in identifying the effectiveness of a particular lithium compound and its dosage, and predicting the duration of its control on ASR expansion. In the present paper, results of new investigations concerning the mechanisms by which lithium nitrate reduces ASR expansion were reported, and a new mechanism to explain the effects of lithium nitrate and the role of calcium in controlling expansion was proposed.

2. Experimental program

2.1. Materials

The materials used for the study reported here included a high-alkali Portland cement (0.91% Na_2Oe), and one commercial vycor glass supplied as thin disks with a dimension of 45 mm × 45 mm × 3~5 mm. The chemical compositions for the above materials were shown in Table 1. Sodium hydroxide and $LiNO_3$ pellets (USP grade) were used as

* Corresponding author. Current affiliation: CTLGroup, Skokie, IL 60077, USA.
E-mail address: xfeng@ctlgroup.com (X. Feng).

0008-8846/$ – see front matter © 2009 Elsevier Ltd. All rights reserved.
doi:10.1016/j.cemconres.2009.07.017

Table 1
Chemical compositions of the materials used in current study (% by mass).

	SiO_2	CaO	Al_2O_3	Fe_2O_3	MgO	Na_2O	K_2O	SO_3	B_2O_3	LOI
Cement	19.7	63.0	5.2	2.0	1.4	0.41	0.76	4.0		2.5
Vycor	96.4		0.5			0			3.0	

the source of Na^+, OH^- and Li^+ ions. Calcium hydroxide powder was used as the calcium source.

2.2. Specimen preparation

2.2.1. Glass disk immersion specimens

For the immersion specimens, glass disks were immersed in different alkaline solutions in sealed plastic containers, and then kept in a temperature controlled room at 38 °C or in an oven at 80 °C. The addition of $Ca(OH)_2$ in some solutions was to simulate concrete pore solutions. After certain ages, the specimens were taken out of solution, washed by deionized distilled water to remove residual NaOH, $LiNO_3$ or $Ca(OH)_2$.

The six different solutions included: 1) 1N NaOH; 2) 1N NaOH plus 0.37N $LiNO_3$; 3) 1N NaOH plus 0.74N $LiNO_3$; 4) 1N NaOH plus supersaturated $Ca(OH)_2$; 5) 1N NaOH plus 0.37N $LiNO_3$ plus supersaturated $Ca(OH)_2$ solution; and 6) 1N NaOH plus 0.74N $LiNO_3$ plus supersaturated $Ca(OH)_2$ solution. Supersaturated $Ca(OH)_2$ was used to compensate for the consumption of calcium ions by the alkali silica reaction.

2.2.2. Glass disk–cement paste sandwich specimens

The vycor glass disk–cement paste sandwich specimens were prepared by putting a thin layer (~5 mm thick) of cement paste with a w/c of 0.5 on the two surfaces. Specimens containing lithium were prepared by adding a certain amount of $LiNO_3$ to the cement paste to produce a 100% standard lithium dose based on the Na_2Oe content of the cement. 100% standard lithium dose provides a Li to alkali molar ratio of [Li]/[Na+K] = 0.74. After 24 h curing at room temperature, specimens were demolded and then were immersed into: 1) 1N NaOH plus saturated $Ca(OH)_2$ solution; and 2) 1N NaOH plus 0.74N $LiNO_3$ plus saturated $Ca(OH)_2$ solutions at 80 °C.

2.3. Methods for analysis

2.3.1. X-ray Diffraction (XRD)

X-ray Diffraction (XRD) technique was selected for the current study. The instrument is Bruker AXS D8 Advance solid-state powder diffraction XRD system.

2.3.2. Scanning Electron Microscopy (SEM)

Scanning Electron Microscopy (SEM) was chosen for the current study. The instrument is EOL JSM6400 Digital SEM with EDAX (Genesis) Energy Dispersive X-ray Analyzer.

2.3.3. Laser Ablation Induction Coupled Plasma Mass Spectrometry (LA-ICP-MS)

In order to supplement the SEM and XRD observations and to get more information about lithium in ASR reaction process, another available analytical technique — Laser Ablation Induction Coupled Plasma Mass Spectrometry (LA-ICP-MS) was employed in the current study. LA-ICP-MS has been widely used as a powerful analytical technique for solid micro sampling analyses. The high sensitivity of the ICP-MS allows small samples to be accurately quantified including almost all the elements in the Periodic Table. Another advantage of this instrument is its spatial resolution can be used to investigate compositional gradients across a sample. Thus the variation in Li, B, Si and Ca concentration with location via a linear traverse across the cement paste–glass interfaces can be examined. The instrument is UP-213 Laser Ablation System coupled with PerkinElmer/SCIEX ELAN 6100 DRCplus ICP-MS.

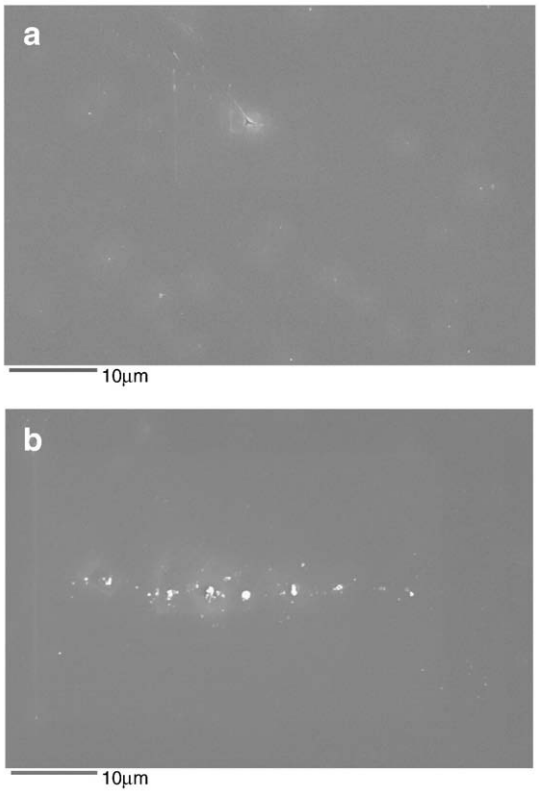

Fig. 1. BSE images of starting glass showing its uniform grains without apparent structure, but contained some cracks and pores as seen in (a), and some impurities as seen in (b).

3. Results

3.1. Specimens at 80 °C

Fig. 1 shows the backscattered secondary electron (BSE) images for the vycor glass disks as supplied. It showed that most of the starting grains was very uniform and without apparent structure, but there were some impurities, and some surface defects such as cracks and pores at some locations. EDS analyses showed there was a bit of deviation between the reported compositions (Table 1) and the testing results (Table 2).

Fig. 2 shows the SEM images of the glass disks after immersed in different alkaline solutions. When it was immersed in only 1N NaOH solution, as shown Fig. 2a, the glass surface showed a worm-like structure with etching sites, which is significantly different from the starting material (Fig. 1a), but no reaction product was found on the glass surface. EDS analyses on the glass surface (as shown in Table 3) showed that the glass compositions were very close to that of the starting material (Table 2). These observations suggested that when

Table 2
EDS analyses for raw glasses (% by mass).

	Na_2O	MgO	Al_2O_3	SiO_2	K_2O	CaO
Vycor 1	0.14	0.2	1.13	95.01	0.09	0.09
Vycor 2	0.12	0.19	1.83	89.52	0.05	1.91
Vycor 3	0.03	0.32	1.63	95.34	0.02	0.03
Vycor 4	0.07	0.27	1.38	92.87	0.07	3.65
Vycor 5[a]	0.13	0.06	1.63	16.38	0.01	75.42
Std dev	0.05	0.06	0.30	2.68	0.03	1.72

[a] Excluded from standard deviation calculation.

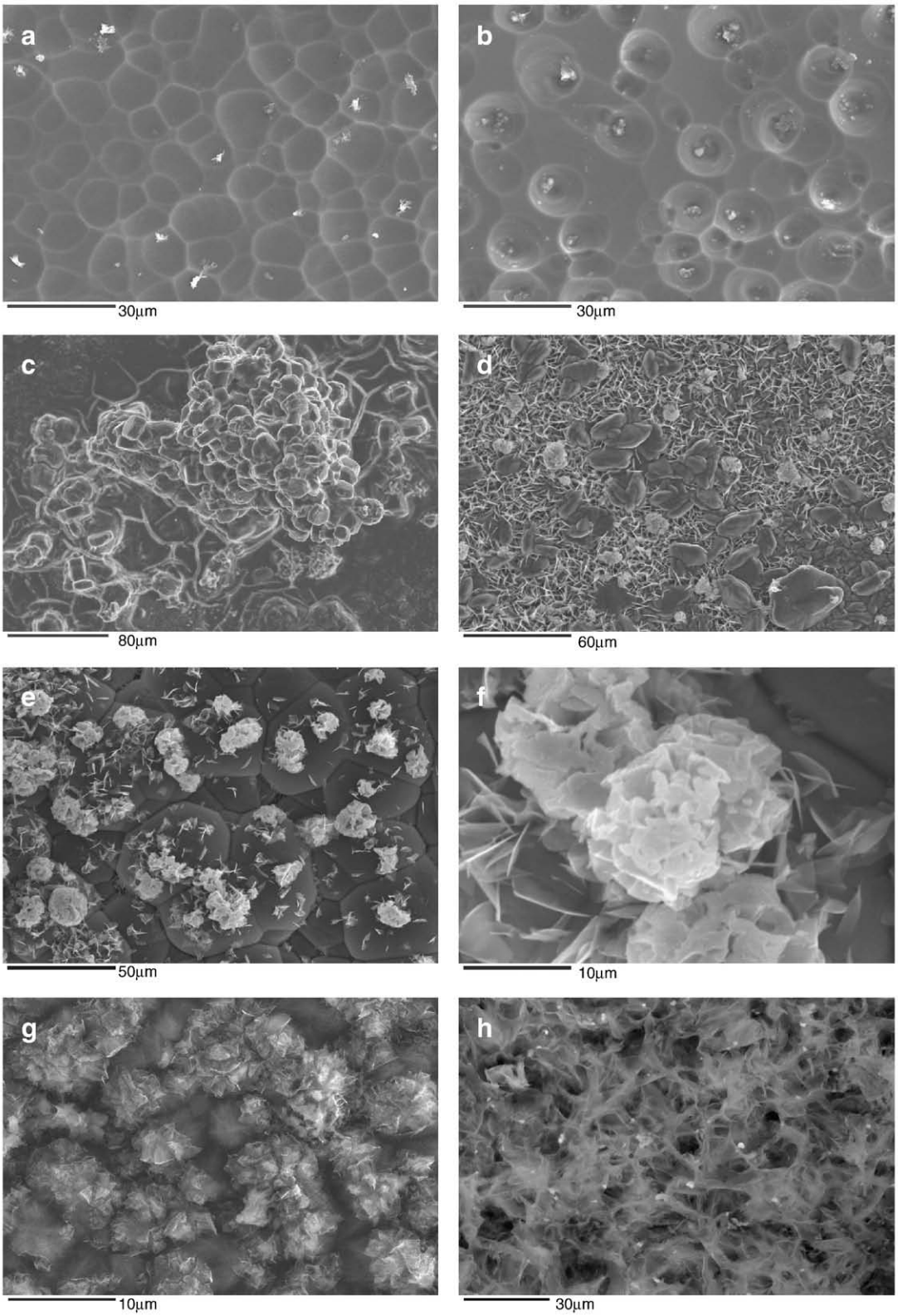

Fig. 2. SEM images of vycor glass disks immersed in alkaline solutions for 28 d at 80 °C. (a) in 1N NaOH, showing the worm-like structure with no reaction product; (b) in 1N NaOH + $Ca(OH)_2$, showing the etching sites without reaction product as well; (c) in 1N NaOH + 0.74N $LiNO_3$, showing a thick layer of Li_2SiO_3 crystals; (d), (e) and (f) in 1N NaOH + 0.74N $LiNO_3$ + $Ca(OH)_2$, showing a matrix of ASR gel and Li–Si crystals as in (d), or the rosette ASR gel sitting on top of Li–Si crystals as in (e), and under high magnification as in (f), gel seen as foils or flakes; (g) in 1N NaOH + 0.37N $LiNO_3$, subhedral Li–Si crystals; (h) in 1N NaOH + 0.37N $LiNO_3$ + $Ca(OH)_2$, surface covered by a layer of ASR gel with C/S of ~0.7.

the glass was immersed in only 1N NaOH solution, the reaction was a simple silica dissolution process, although the glass has been severely attacked by the alkalis.

As shown in Fig. 2b, with the addition of $Ca(OH)_2$, surprisingly the glass surface had a very similar morphology to the one in the absence of $Ca(OH)_2$. Again, no reaction product was found on the glass surface.

Table 3
ASR gel compositions from EDS analysis.

	Li-low Ca-Na-Si gels	Li-high Ca–Na–Si gels	Ca–Na–Si gels
C/S by mole	0.00–0.21	>0.21	0.26–0.78
SiO_2, wt.%	35–78	30–43	32–79
CaO, wt.%	1.9–14	20–26	16–35
Na_2O, wt.%	0.3–9	0.2–2.4	0.4–22

EDS analyses revealed that the glass compositions were very close to that of the starting material as well. It seemed that the addition of Ca $(OH)_2$ did not have any influence on the reaction process. However, it was noted that some solid materials precipitated in the solution. After taking the glass specimens out, the solutions were filtered to collect the solid materials that formed in the solutions. The solid materials were then analyzed by XRD. Results are shown in Fig. 5.

When immersed in 1NNaOH + 0.74N $LiNO_3$, as shown in Fig. 2c, the whole glass surface was completely covered by a very thick layer of crystalline material with 64–72% SiO_2 by mass from EDS analyses. Before carbon coating for SEM examinations, the same piece disk was taken to run an XRD analysis. It confirmed this crystalline deposit was Li_2SiO_3, as shown in Fig. 3.

With the addition of $Ca(OH)_2$, as shown in Fig. 2d, the glass surface was covered either by a matrix of white rosette crystalline ASR gel products and darker gravel-like phase with 64–70% SiO_2 which might be Li–Si crystals (Fig. 2d), or a thick darker layer of Li–Si crystals with some white rosette gels randomly sitting on the top (Fig. 2e). It seemed the darker layer served as the foundation and base for the gel products. Under higher magnification (Fig. 2f), the gel products consisted of foils or flakes, that are similar to the early conventional C–S–H [21]. But the EDS analyses in Fig. 4 showed they had a much lower Ca content range than conventional C–S–H. Again, it should be noted the EDS analyses could not reveal the Li content in these gels.

When lithium dose in the solution was reduced to half, in the absence of $Ca(OH)_2$ (Fig. 2g), the glass surface was also covered by a thick layer of Li–Si crystals. But the crystals were subhedral without a full external crystal surface, and were not as angular as they were in the solution with 100% lithium dose. With the addition of $Ca(OH)_2$ (Fig. 2h), the glass surface was completely covered by white lamellar crystalline gel products, and no Li–Si crystal was found at the whole surface. From the EDS results in Fig. 4, these white gels were found to contain significantly higher Ca content than the gels found in the specimens immersed in 100% Li solution.

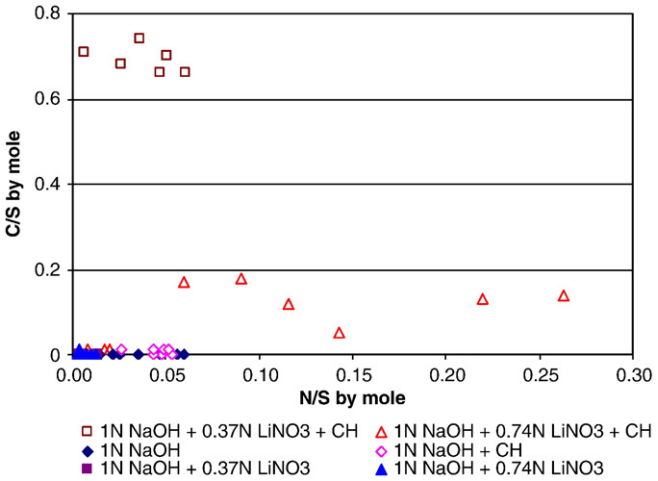

Fig. 4. EDS analyses of Vycor glass disks immersed for 28 d at 80 °C.

Fig. 5 shows the XRD results for the solid residues obtained from glass immersion tests. When immersed in solely NaOH solution, the solution was clear, no solid residue was left in it, suggesting no new phase forming in this process. With $Ca(OH)_2$, a crystalline phase was identified as $Ca_{4.5}Si_6O_{15}(OH)_3 \cdot 2H_2O$. Is this the only reaction product in the system? Maybe possible or maybe not, because the XRD analysis cannot detect amorphous phase. For the residue obtained from solution containing 1N NaOH and 0.74N $LiNO_3$, as expected, Li_2SiO_3 was found. With both $LiNO_3$ and $Ca(OH)_2$, interestingly, only $Ca(OH)_2$ was left in the solution, which means both the Li–Si crystal and gel products seen on the glass surface by SEM (Fig. 2d, e, f) were strongly bound at the glass surface. This proves that the low Ca gel phase is very stable, with little or no mobility, thus having a strong binding with the glass surface.

Fig. 6 shows the SEM images of vycor glass–cement paste sandwich specimens immersed in different alkaline solutions. In the control samples, massive cracked ASR gel could be easily found at the interface between the glass and cement paste. These gels had a comparable Ca content range to that of the glass immersion specimens in solution with

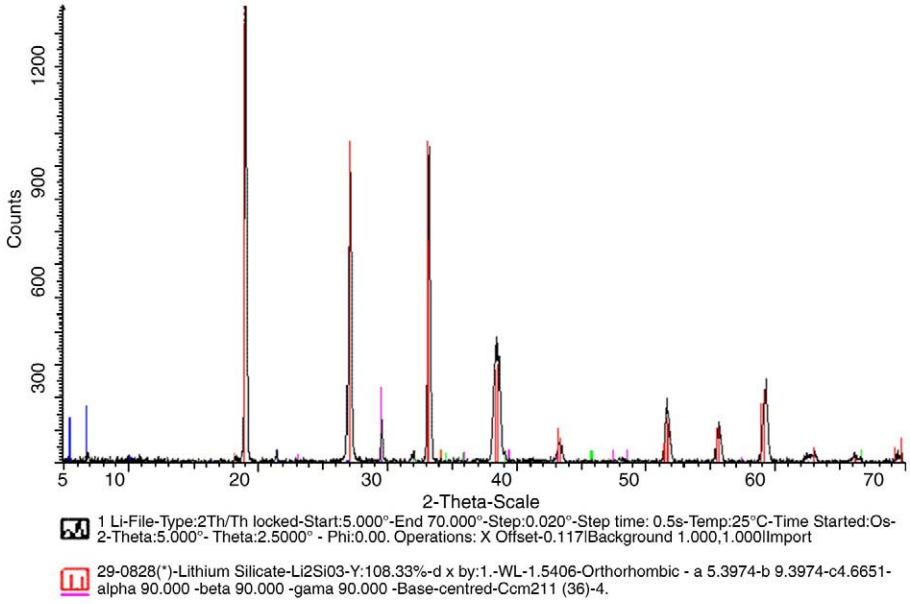

Fig. 3. XRD spectra of the surface of vycor glass disk immersed in 1N NaOH + 0.74N $LiNO_3$ solution for 28 d at 80 °C, showing a pure Li_2SiO_3 crystal.

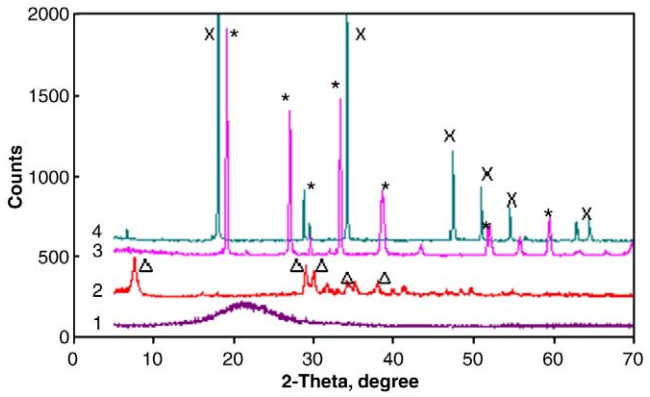

Fig. 5. XRD spectra for the solid residues obtained from the glass immersion tests. 1) starting glass powder; 2) in 1N NaOH + $Ca(OH)_2$; 3) in 1N NaOH + 0.74N $LiNO_3$; 4) in 1N NaOH + 0.74N $LiNO_3$ + $Ca(OH)_2$. X portlandite, * Li_2SiO_3 , Δ $Ca_{4.5}Si_6O_{15}(OH)_3 \cdot 2H_2O$.

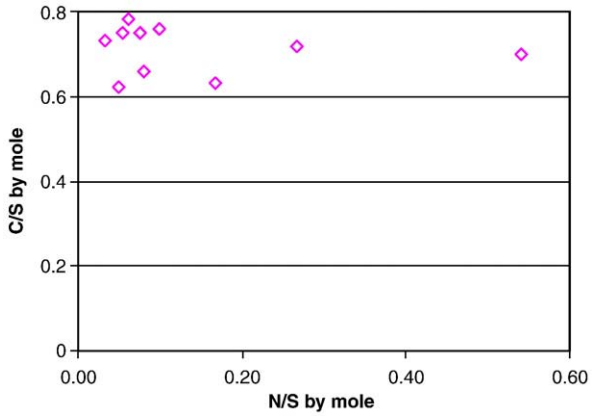

Fig. 7. EDS analyses of Vycor glass–cement paste specimens for 28 d at 80 °C.

50% lithium dose (Fig. 7). This provided a powerful evidence for Hansen's osmotic theory [22], in which, the hardened cement paste surrounding the aggregate particle works as a semi-permeable membrane. It allows the passage of the alkaline solution into the aggregate and does not permit the aqueous sodium silicate to pass out. In the lithium-containing specimen, the interface between the glass and cement paste was not clear, and no Li–Si crystal and gel product could be identified.

Fig. 8 are the LA-ICP-MS test results showing the elemental distributions along the line starting from cement paste to glass disk or vice versa for the vycor glass disk–cement paste sandwich specimens with 100% lithium immersed in 1N NaOH + 0.74N $LiNO_3$ + $Ca(OH)_2$ solution for 28 d at 80 °C. It can be seen that near the glass surface

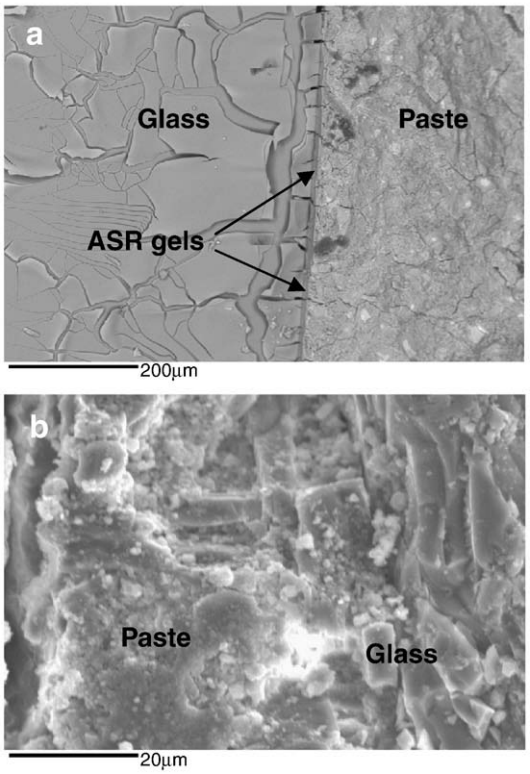

Fig. 6. SEM images of glass–cement paste sandwich specimens cured for 28 d at 80 °C. (a) control specimen without lithium, showing massive ASR gels at the interface between the glass and cement paste; (b) sample containing 100% lithium dose, no Li–Si crystal and gel product was found at the interface.

area, there was a layer which was very rich in Li and Si, this might correspond to the Li–Si crystals observed by SEM and XRD. Then near by this layer toward the cement paste, the Ca content began increasing, which appeared to form another layer which was rich in Li, Si and some Ca, this might reflect to the ASR gel products with lower amount of Ca. These findings further suggested that the ASR gel contained certain amount of Li.

3.2. Specimens at 38 °C

Fig. 9 shows the SEM images for the vycor glass disks immersed in different alkaline solutions for 120 d at 38 °C. When immersed in only 1N NaOH solution, the glass showed no change in shape or even roughening of the surface. While with $Ca(OH)_2$ (Fig. 9b), a typical amorphous ASR gel product was observed, which appeared to exfoliate from the glass surface. EDS analyses in Fig. 10 showed they had a much higher Ca content with a C/S ratio of 0.26–0.70. In the presence of $LiNO_3$ (Fig. 9c), again, the only phase was Li–Si crystal with small prism-like morphology. With the addition of $Ca(OH)_2$ (Fig. 9d), a matrix of angular crystals and net gel products covered the entire glass surface. EDS analyses showed that the crystals have similar SiO_2 contents to the Li_2SO_3 crystals by XRD found in vycor glass disk immersed in 1NaOH + 0.74N $LiNO_3$ solution for 28 d at 80 °C, suggesting the crystals were probably Li_2SiO_3. EDS also showed that the gel had a much lower Ca content than the gel in the absence of lithium (Fig. 9b).

4. Discussions

4.1. ASR gel products in the presence of lithium

The lithium-bearing ASR gel is another type of ASR reaction product yielded in the presence of lithium. From the SEM images, it is found that there are three different forms of the Li–Ca–Na–Si gels encountered in the current study based on their morphology: rosette-like (Fig. 2f), lamellar (Fig. 2h), and amorphous (Fig. 9d). These forms are also the most commonly observed gel morphologies for conventional ASR gel products [23]. According to the C/S ratio of these gels, they can be further divided into two categories: one is low Ca content gel; the other is high Ca content gel. The first type of gels was mostly found with the addition of lithium at 100% standard lithium dose; while the second category was mainly observed in specimens with 50% lithium dose.

Table 3 summarizes the EDS analysis results for all the ASR gels observed, including the gels formed in the absence of lithium. It can be seen that the gel compositions changed in a wide range even for the same type of gel. Unfortunately, no quantitative information about the lithium content in those gels is available due to the inaccessibility of suitable analytical techniques.

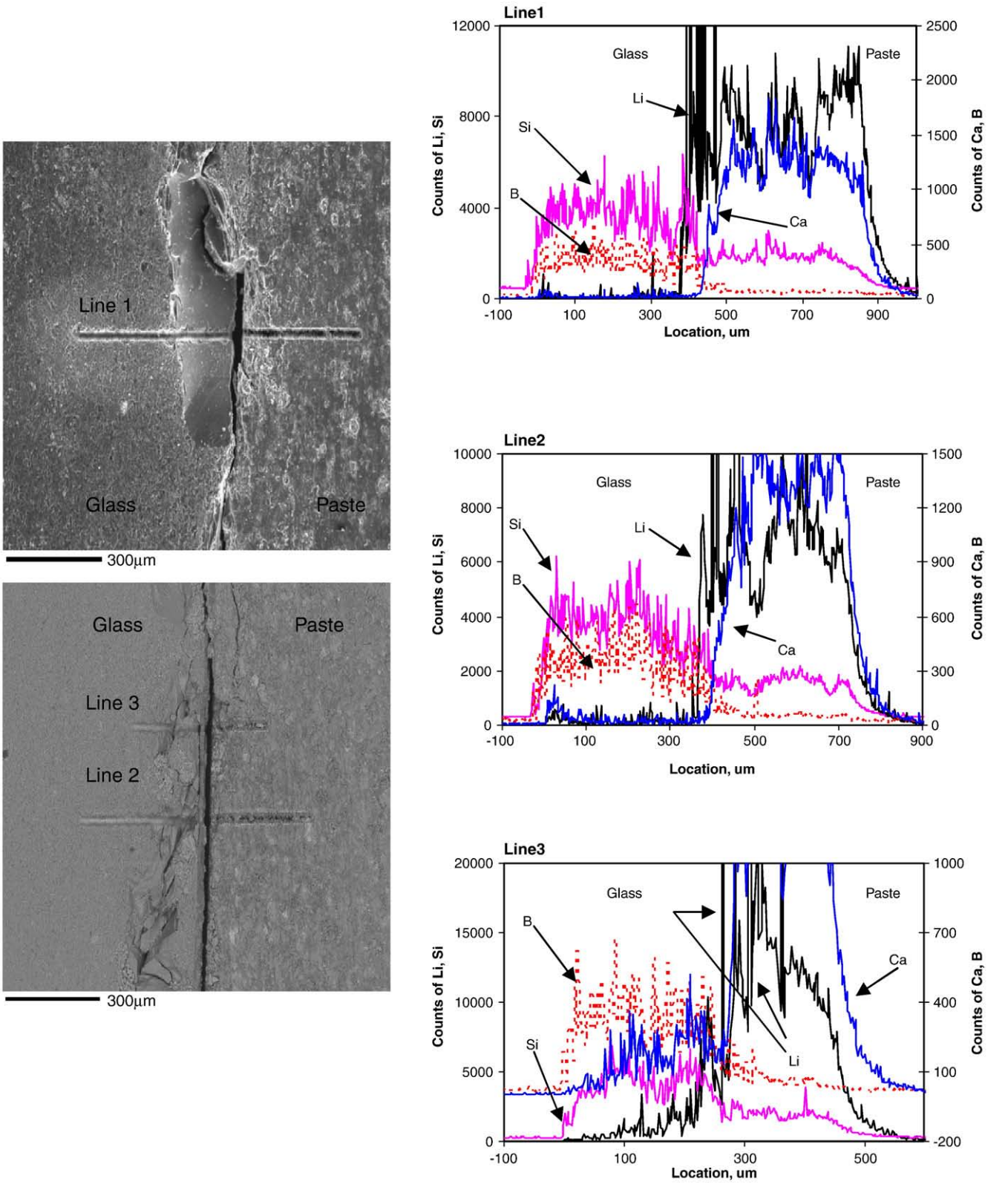

Fig. 8. Elemental distributions of the glass disk–cement paste sandwich specimens with 100% Li dose cured for 28 d at 80 °C.

4.2. Mechanism by which $LiNO_3$ controls expansion due to ASR

Based on the previous discussion, a mechanism for the efficacy of $LiNO_3$ in controlling ASR-induced expansion can be established as below: The suppressive effects of $LiNO_3$ on ASR expansion can be explained by the formation of a layer of Li–Si crystals intimately at the reactive SiO_2 particle surface which serves as a diffusion barrier and protective layer to keep the reactive aggregate particles from further attack by alkalis; and the formation of Li-bearing low-Ca ASR gel products with a C/S ratio below 0.2, which have denser gel structure,

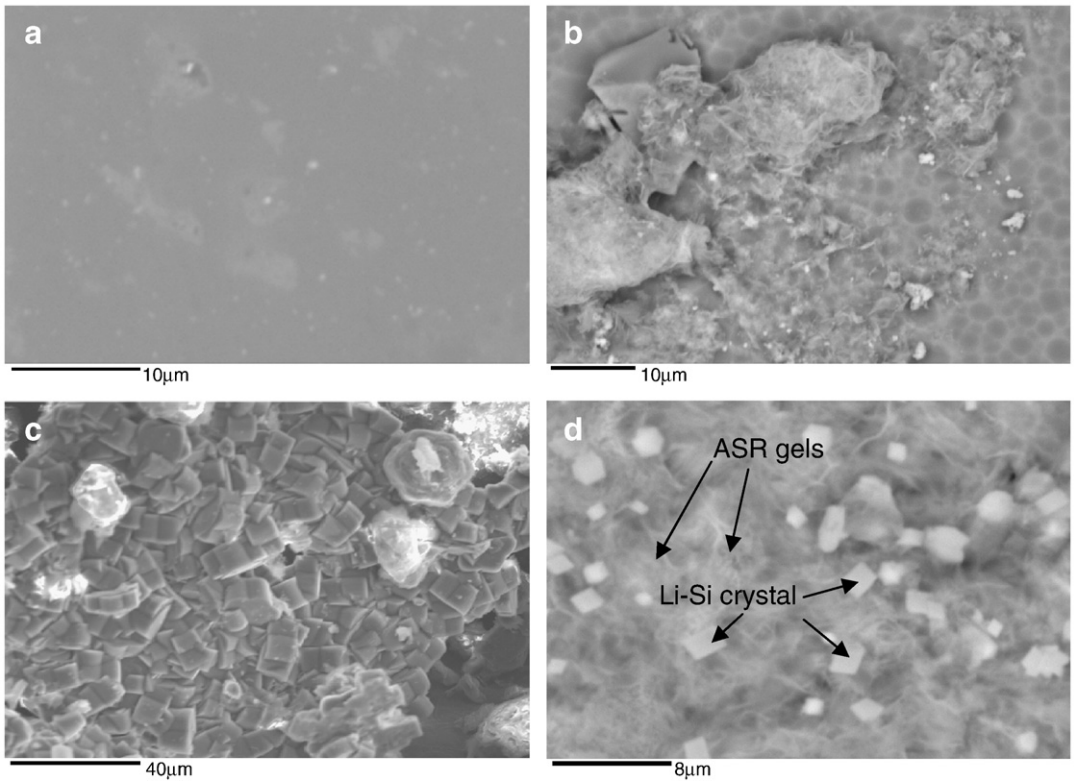

Fig. 9. SEM images of vycor glass disks immersed in alkaline solutions for 120d at 38 °C. (a) in 1N NaOH, no significant reaction at the glass surface; (b) in 1N NaOH + $Ca(OH)_2$, a typical ASR gel was found with a higher C/S ratio of 0.26–0.70 ; (c) in 1N NaOH + 0.74N $LiNO_3$, showing a thick layer of Li–Si crystals; (d) in 1N NaOH + 0.74N $LiNO_3$ + $Ca(OH)_2$, showing a matrix of ASR gel and Li–Si crystals.

stronger bound with the aggregate particles, and lower mobility than conventional ASR gel. The formation of Li–Si crystal is essential, while the formation of the Li–Ca–Na–Si gel is unavoidable. These two phases either form a dense matrix with the Li–Si crystal serving as the framework, and the gel filling in the void space, or the Li–Si crystal serving as the foundation to completely cover the entire reactive aggregate surface, and the gel sitting on top of these crystal particles, as shown in Fig. 11. Thus with sufficient thickness of the reaction products, less and less OH^- ions can pass through the diffusion barriers. As a result, the alkali silica reaction and its induced expansion will be completely suppressed.

The Li-bearing low-Ca ASR gels may have a dense and rigid structure, thus having low capacity to absorb moisture from the surrounding paste, and exhibiting a non-swelling property.

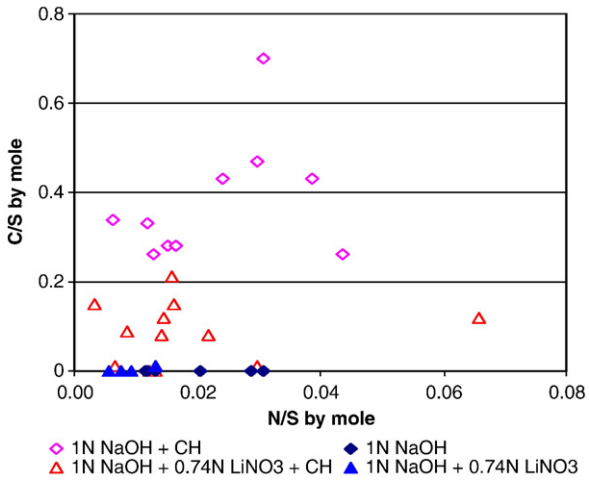

Fig. 10. EDS analyses of Vycor glass disks immersion for 120 d at 38 °C.

In the following parts, this mechanism will be applied to explain several issues encountered in the application of $LiNO_3$ to prohibit ASR expansion.

4.3. The ASR reaction process in the presence of lithium

When pertaining to the addition of lithium against ASR, most researchers used to think the efficacy of lithium were greatly affected by the competition between lithium and sodium on the consumption of reactive SiO_2. The work conducted here can provide a clear answer about this competition and about the reaction process with the presence of lithium.

In a related study on the diffusion of Li and Na in cement paste, mortars containing inert sand and reactive aggregates showed that Na ions had a greater effective diffusion coefficient than that of Li ions, thus Na ions could reach the aggregate particle surface first. However, NaOH did not yield a solid reaction product with reactive SiO_2. It only simply dissolved SiO_2, as evidenced in the current study. Thus the first three

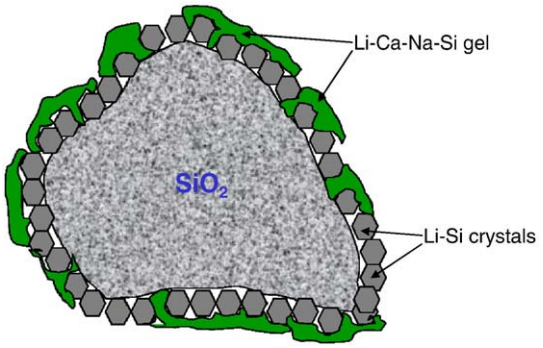

Fig. 11. Schematic diagram of reaction system in the presence of lithium.

steps of the reaction process are the same as the process without lithium [24]. Then, the ASR reaction process with the presence of lithium will be comprised of following five sequences.

1) The dissolution of silica by hydroxyl attack.
2) Reaction of surface silanol (Si–OH) groups with hydroxyl ions (OH^-) in the solution to further promote dissolution;
3) Binding of the alkali cations (Na^+, K^+, Li^+) and calcium cations (Ca^{2+}) at negatively charged sites on the silicate surface;
4) Formation of Li–Si crystals by silicate species in solution with lithium ions in solution;The Li–Si crystal probably is the first solid product formed in this system, although Na ions reached the SiO_2 particles earlier than Li ions.
5) Formation of Li-bearing ASR gels;This step may occur simultaneously with the formation of Li–Si crystals.
6) Cease of alkali silica reaction

When the SiO_2 is completely covered by Li–Si crystals or the dense matrix of Li–Si crystals and Li-bearing ASR gels, less and less OH^- ions penetrate through these product layers, eventually the reaction will come to an end, consequently, the expansion will be stopped as well.

5. Conclusions

Based on the above study, a mechanism for the suppressive effects of $LiNO_3$ against ASR was proposed as follows: The suppressive effects of $LiNO_3$ on ASR expansion can be explained by the formation of a layer of Li–Si crystals intimately at the reactive SiO_2 particle surface which serves as a diffusion barrier and protective layer to keep the reactive aggregate particles from further attack by alkalis; and the formation of Li-bearing low-Ca ASR gel products with a C/S ratio below 0.2, which have a denser gel structure, stronger bound with the aggregate particles, and lower mobility than conventional ASR gel. These two phases either form a dense matrix with the Li–Si crystal serving as the framework, and the gel filling in the void space, or the Li–Si crystal serving as the foundation to completely cover the entire reactive aggregate surface, and the gel sitting on top of these crystal particles. Thus with sufficient thickness of the reaction products, less and less OH^- ions can pass through the diffusion barriers. As a result, the alkali silica reaction and its induced expansion will be completely suppressed.

References

[1] W.J. McCoy, A.G. Caldwell, New approach to inhibiting alkali-aggregate expansion, Journal of the American Concrete Institute 22 (1951) 693–706.
[2] M. Lowrence, H.E. Vivian, The reactions of various alkalis with silica, Australian Journal of Applied Science 12 (1961) 96–103.
[3] D.C. Stark, Lithium salt admixtures — an alternative method to prevent expansive alkali–silica reactivity, Proceedings of the 9th International Conference on Alkali-Aggregate Reaction, 1992, pp. 1017–1025.
[4] D.C. Stark, B. Morgan, P. Okamoto, S. Diamond, Eliminating or Minimizing Alkali–silica Reactivity, 1993 No. SHRP-C-343.
[5] T. Sakaguchi, M. Takakura, A. Kitagawa, T. Hori, F. Tomozawa, M. Abe, The inhibitive effect of lithium compounds on alkali–silica reaction, Proceedings of the 8th International Conference on Alkali-Aggregate Reaction, 1989, pp. 229–234.
[6] Y. Ohama, K. Demura, M. Kakegawa, Inhibiting ASR with chemical admixtures, Proceedings of the 8th International Conference of Alkali – Aggregate Reaction, 1989, p. 253.
[7] J.S. Lumley, ASR suppression by lithium compounds, Cement and Concrete Research 27 (1997) 235–244.
[8] M.D.A. Thomas, B.Q. Blackwell, K. Pettifer, Suppression of damage from alkali silica reaction by fly ash in concrete dams, Proceedings of the 9th International Conference on Alkali-Aggregate Reaction in Concrete, 1992, pp. 1059–1066.
[9] V.S. Ramachandran, Alkali-aggregate expansion inhibiting admixtures, Cement and Concrete Composites 20 (1998) 149–161.
[10] S. Diamond, Unique response of $LiNO_3$ as an alkali–silica reaction-prevention admixture, Cement and Concrete Research 29 (1999) 1271–1275.
[11] M.D.A. Thomas, R. Hooper, D. Stokes, Use of lithium-containing compounds to control expansion in concrete due to alkali–silica reaction, Proceedings of the 11th International Conference on Alkali-Aggregate Reaction, 2000, pp. 783–792.
[12] C.L. Collins, J.H. Ideker, G.S. Willis, K.E. Kurtis, Examination of the effects of LiOH, LiCl, and $LiNO_3$ on alkali–silica reaction, Cement and Concrete Research 34 (2004) 1403–1415.
[13] C. Tremblay, M.A. Berube, B. Fournier, M.D.A. Thomas, D.B. Stokes, Performance of lithium-based products against ASR: application to Canadian reactive aggregates, reaction mechanisms, and testing, Proceedings of the 12th International Conference on Alkali-Aggregate Reaction, 2004, pp. 668–677.
[14] P.W.J.G. Wijnen, T.P.M. Beelen, J.W. de Haan, C.P.J. Rummens, L.J.M. van de Ven, R.A. van Santen, Silica gel dissolution in aqueous alkali metal hydroxides studied by ^{29}Si-NMR, Journal of Non-Crystalline Solids 109 (1989) 85–94.
[15] K. Kurtis, P.J.M. Monteiro, Chemical additives to control expansion of ASR gels: proposed mechanisms of control, Journal of Material Science 38 (2003) 2027.
[16] K. Kurtis, P.J.M. Monteiro, W. Meyer-Ilse, Examination of the effect of LiCl on ASR gel expansion, Proceedings of the 11th International Conference on Alkali-Aggregate Reaction, 2000, pp. 51–60.
[17] M. Prezzi, P. Monteiro, G. Sposito, The ASR: Part I. use of the double-layer theory to explain the behavior of the reaction product gels, Journal of ACI Materials 94 (1997) 10.
[18] M.D.A. Thomas, unpublished data, (2003).
[19] K. Folliard, M.D.A. Thomas, B. Fournier, K. Kurtis, J. Ideker, Interim Recommendations for the Use of Lithium to Mitigate or Prevent ASR, 2006 Publication No. FHWQ-HRT-06-073.
[20] X. Feng, M.D.A. Thomas, T.W. Bremner, B.J. Balcom, K.J. Folliard, Studies on lithium salts to mitigate ASR-induced expansion in new concrete: a critical review, Cement and Concrete Research 35 (2005) 1789–1796.
[21] H.F.W. Taylor, Cement Chemistry, 2nd editionThomas Telford Publishing, 1997 124 pp.
[22] W.C. Hansen, Studies relating to the mechanism by which the alkali-aggregate reaction proceeds in concrete, Journal of the American Concrete Institute 15 (1944) 213–227.
[23] Advisory Circular, Handbook for identification of alkali–silica reactivity in airfield pavements, U.S. Department of Transportation, 2004.
[24] L.S.D. Glasser, N. Kataoka, The chemistry of alkali-aggregate reactions, Proceedings of the 5th International Conference on Alkali-Aggregate Reaction, 1981, P. S252/23.